Polymorphism of *N*-Alkanols: 1-Heptadecanol, 1-Octadecanol, 1-Nonadecanol, and 1-Eicosanol

L. Ventolà, M. Ramírez, T. Calvet,* X. Solans, and M. A. Cuevas-Diarte

Departament de Cristallografia, Mineralogia i Dipòsits Minerals, Facultat de Geologia, Universitat de Barcelona, Martí i Franquès s/n, E-08028 Barcelona, Spain

P. Negrier and D. Mondieig

Centre de Physique Moléculaire Optique et Hertzienne, UMR 5798 au CNRS Université Bordeaux I, France

J. C. van Miltenburg and H. A. J. Oonk

Chemical Thermodynamics Group, Faculty of Chemistry, Debye Institute, Utrecht University, Utrecht, The Netherlands

Received January 17, 2001. Revised Manuscript Received October 22, 2001

The polymorphism of 1-heptadecanol ($C_{17}H_{35}OH$), 1-octadecanol ($C_{18}H_{37}OH$), 1-nonadecanol ($C_{19}H_{39}OH$), and 1-eicosanol ($C_{20}H_{41}OH$) has been studied by X-ray powder diffraction, differential scanning calorimetry (DSC), Raman scattering, and infrared spectroscopy (IR). At room-temperature two monoclinic forms, β and γ, are observed. For the *n*-alkanols with an even number of carbons the stable form is γ, whereas β is the stable form for the *n*-alkanols with an odd number of carbons. On heating, these phases transform to a monoclinic, rotator form R'_{IV} at a few degrees below the melting point. A metastable β form is obtained by quenching from the melt for 1-octadecanol and 1-eicosanol, which is isostructural with the β-phase of the odd alkanols. Cell parameters, temperatures, and enthalpies of the transitions are reported.

I. Introduction

This study is a part of the research on elaboration, characterization, prediction and application of molecular alloys, which is carried out by the "Réseau Européen sur les Alliages Moléculaires" (REALM). The work presented here is the first part of a general study on the solid-state miscibility in the *n*-alkanol family. Alkanols are compounds with a high heat of fusion. This implies that the substances and their alloys are promising candidates for storing thermal energy, one of the reasons for our study. We present the polymorphic behavior of 1-heptadecanol ($C_{17}H_{35}OH$), 1-octadecanol ($C_{18}H_{37}OH$), 1-nonadecanol ($C_{19}H_{39}OH$), and 1-eicosanol ($C_{20}H_{41}OH$), until now only partially described. A complementary approach including X-ray powder diffraction, differential scanning calorimetry (DSC), Raman scattering, and infrared spectroscopy (IR) was used.

Normal alkanols are among the simplest of the substituted hydrocarbons. A single −OH group replaces a hydrogen atom at one end of the aliphatic chain. For the *n*-alkanols with between 12 and 20 carbon atoms, two ordered monoclinic phases at room temperature, named γ and β, have been described.[1−9] The principle of a common structural description is summed up elsewhere.[10] It is based on the assumption that the presence of long alkanol chains packed in a regular and parallel crystallographic array would be described in the base of a sub-cell that defines the repeating unit of the whole structure. This three-dimensional subcell is defined by three axes: c_s for the translation between equivalent positions within a chain and a_s and b_s for the lateral translations. When the long axis of the molecule tilts over the shortest axis of the rectangular planar subcell, the modification is called γ. If the long axis of the molecule tilts over the longest axis of the rectangular subcell, the modification is called β. The γ-phase is more frequent in even *n*-alkanols, the β-phase in odd *n*-alkanols. We will retain the same nomenclature for these phases. Before melting, these ordered phases transform to rotator phases where the molecules rotate around their long axis and different conformational defects appear.[11] These phases are designed by similarity to the alkanes: R_{II}, R_{IV}, and R_V.[12−18] However, since

* To whom correspondence should be addressed.

(1) Tanaka,K.; Seto, T.; Watanabe, A.; Hayashida, T. *Bull. Inst. Chem. Res. Kyoto Univ*. **1959**, *37*, 281.
(2) Abrahamsson, S.; Larsson, G.; von Sydow, E. *Acta Crystallogr*. **1960**, *13*, 770.
(3) Watanabe, A. *Bull. Chem. Soc. Jpn*. **1961**, *34*, 1728.
(4) Watanabe, A. *Bull. Chem. Soc. Jpn*. **1963**, *36*, 336.
(5) Seto,T. *Mem. Coll. Sci. University Kyoto A* **1962**, *30*, 89.
(6) Precht, D. *Fette Seifen Anstrichm*. **1976**, *4*, 145.
(7) Precht, D. *Fette Seifen Anstrichm*. **1976**, *5*, 189.
(8) Fujimoto, K.; Yamamoto, T.; Hara, T. *Rep. Prog. Polym. Phys. Jpn*. **1985**, *28*, 163.
(9) Michaud, F.; Ventolà, L.; Calvet, T.; Cuevas-Diarte, M. A.; Solans, X. Font-Bardia, M. *Acta Crystallogr. C* **2000**, *56*, 219.
(10) Small, D. M. *Handbook of Lipid Research*; Plenum Press: New York, 1986.
(11) Ishikawa, S.; Ando, I. *J. Mol. Struct*. **1993**, *291*, 183.

10.1021/cm011010h CCC: $22.00
Published on Web 01/23/2002

the isostructural relationships between the rotator phases of alkanes and alkanols have not yet been studied, we will adopt different notations (R'_{II}, R'_{IV}, and R'_{V}).

At room temperature the crystal structure of $C_{18}H_{37}OH$ is known from previous studies[5,8] and the crystal structure of $C_{20}H_{41}OH$ has been determined by our group.[9] Both substances present a monoclinic phase γ with space group $C2/c$ and eight molecules in the unit-cell. All C−C bonds of the polymethylene chain show an anti-periplanar (trans) conformation, with a slight difference from the ideal 180° value in the C−C bonds close to the hydrogen bond. The chains are parallel to [1 0 $\bar{6}$] in 1-octadecanol and [3 0 $\overline{20}$] direction in 1-eicosanol. The molecules are packed by OH···OH hydrogen bonds in layers parallel to (100) plane. The crystal structure of the β-phase for $C_{17}H_{35}OH$ is known.[5] This phase is also monoclinic with space group $P2_1/c$ and eight molecules in the unit-cell. The structure contains two molecules in the asymmetric unit, each one is a different rotational isomer and disposed alternatively: the first isomer is an all-trans conformer (similar to γ-phase) while the second isomer has all C−C−C−C torsion angles in trans-form and the C−C−C−O torsion angle in gauche form. The molecules are packed by OH···OH hydrogen bonds in layers parallel to (001) plane. To compare the two phases more easily, in this paper we have changed the conventional space group $C2/c$ to $A2/a$. In this case, the molecules in γ-phase are also packed in layers parallel to (001) plane with a greater tilt angle than in β-phase.

Precht[6] and Dorset[19] characterized a β-phase of $C_{18}H_{37}OH$ and $C_{20}H_{41}OH$. This phase was also observed by Tasumi et al.[20] using infrared spectroscopy. Dorset studied the β-phase of $C_{18}H_{37}OH$ from electron diffraction and image data. He concluded that the β-form is orthorhombic, obtaining values for a- and b-cell parameters, and suggested that gauche forms were involved in the C_1-C_2 single bond, where C_1 is the carbon linked to the OH group. Precht studied both compounds with electron and X-ray diffraction and concluded that the β-form is monoclinic, obtaining values for the cell parameters and also suggesting the presence of the same gauche form.

The structure of the rotator phases is not clear. In early papers,[21] these phases were characterized as a hexagonal phase similar to the R_{II} phase of *n*-alkanes. Seto[5] studied the rotator phases of $C_{17}H_{35}OH$ and $C_{18}H_{37}OH$ by X-ray diffraction on single crystals using photograph techniques and only obtained the cell parameters, with a probable space group $C2/m$ and a tilt angle of the molecular axis of 83° and 83.5°, respectively. The X-ray analysis, however, did not give information about the local structure. Ishikawa,[11] by ^{13}C NMR spectroscopy, found that the behavior of the internal CH_2 carbons of the rotator phase of 1-octadecanol is identical to that of orthorhombic *n*-alkanes, which is inconsistent with the monoclinic symmetry found by Seto.[5]

II. Experimental Procedures

Materials. The four *n*-alkanols were purchased from Fluka with a purity grade certified ≥99%. The analyses were done on a commercial product, on a product recrystallized from acetone and ether solutions, and on molten substances, after a quenching in a liquid nitrogen bath and crystallizing with a slow rate cooling process.

X-ray Powder Diffraction Analysis. Two kinds of powder-diffraction analysis were performed at different temperatures: one with a Guinier-Simon camera and another with a Siemens D500 diffractometer. The first instrument works in transmission mode using Cu Kα radiation, with a quartz crystal as the primary monochromator. The sample was mounted on a rotating sealed capillary of 0.5 mm diameter, perpendicular to the X-ray radiation beam. The window width used was 1.5 mm. The sample was heated and cooled several times at 0.5 K·min^{-1}. The continuous evolution of the X-ray pattern is registered on a photographic film, which is moved perpendicularly to the beam at a constant rate of 1 mm·h^{-1}.

The second instrument, the Siemens D-500 diffractometer, was used working in the Bragg−Brentano geometry, using Cu Kα radiation and a secondary monochromator. Patterns were collected at constant temperature using an Anton PAAR TTK camera with a heating rate of 0.02 K·s^{-1} and 5 min of stabilization time. The measurements were taken from room temperature until the melting. The patterns were scanned with a step size of 0.025°; step time of 10 s and a 2θ range of 1.6−60°. Cell parameters were refined from Siemens diffraction data with the FULLPROF computer program[22] using a profile matching option.

The measurements for the quenched samples were made at 298 K after 1 h, 1 week, 1 month, and 3 months from the preparation of the sample. Samples were also measured in a heating process, each degree from two degrees below the first transition up to the melting point.

Differential Scanning Calorimeter (DSC). Calorimetric measurements were made with a Perkin-Elmer DSC-7 calorimeter. In sealed aluminum pans the samples were heated, cooled and heated again, with two different rates, at 2 and 0.1 K·min^{-1}. The temperature range was from 273 K to the liquid phase. For each one of the alkanols, six samples were analyzed, with weights between 3.9 and 4.1 mg. The instrument was calibrated using the known fusion temperature and enthalpy of indium and fusion temperature of *n*-decane. The random part of the uncertainties was estimated using the Student's method, with a 95% threshold of reliability. The uncertainties of temperatures and heat-flow calibration coefficient for the DSC were ±0.2 K and ±2%, respectively.

Raman Scattering. Polarized Raman spectra were taken on powdered samples using a Jobin Yvon T64000 spectrometer and an argon-ion laser excitation. The detector used was a Control Data CDC. The spectra were recorded with the 514.5 nm line used with a light power equal to 1.05 W for processing at variable temperatures and 3.30 W for measurements at 298 K. All spectra were calibrated against selected neon lines. The measured range was 17.5−1700 cm^{-1}. All the spectra at 298 K were measured in macro-Raman, whereas the spectra at different temperatures (on the heating and on the cooling processes) were measured in micro-Raman, with a Mettler

(12) Maroncelli, M.; Qi, S. P.; Strauss, H. L.; Snyder, R. G. *J. Am. Chem. Soc.* **1982**, *104*, 6237.
(13) Sirota, E. B.; King, H. E.; Singer, D. M.; Shao, H. H. *J. Chem. Phys.* **1993**, *98*, 5809.
(14) Sirota, E. B.; King, H. E.; Shao, H. H.; Singer, D. M. *J. Phys. Chem.* **1995**, *99*, 798.
(15) Sirota, E. B.; Wu, X. Z. *J. Chem. Phys.* **1996**, *105*, 7763.
(16) Espeau, P.; Roblés, L.; Mondieig, D.; Haget, Y.; Cuevas-Diarte, M. A.; Oonk, H. A. J. *J. Chim. Phys.* **1996**, *93*, 1217.
(17) Roblés, L.; Mondieig, D.; Haget, Y.; Cuevas-Diarte, M. A. *J. Chim. Phys.* **1998**, *95*, 92.
(18) Oonk, H. A. J.; Mondieig, D.; Haget, Y.; Cuevas-Diarte, M. A. *J. Chem. Phys.* **1998**, *108* (2), 715.
(19) Dorset, D. L. *Chem. Phys. Lipids* **1979**, *23*, 337.
(20) Tasumi, M.; Shimanouchi, T.; Watanabe, A.; Goto, R. *Spectrochim. Acta* **1964**, *20*, 629.
(21) Frede, E.; Precht, D. *Kiel. Milchwirtsch. Forschungsber.* **1974,** *26*, 325.
(22) Rodríguez-Carvajal, J. *FULLPROF 98 Program*; Laboratoire Leon Brillouin, Paris, France, 1998.

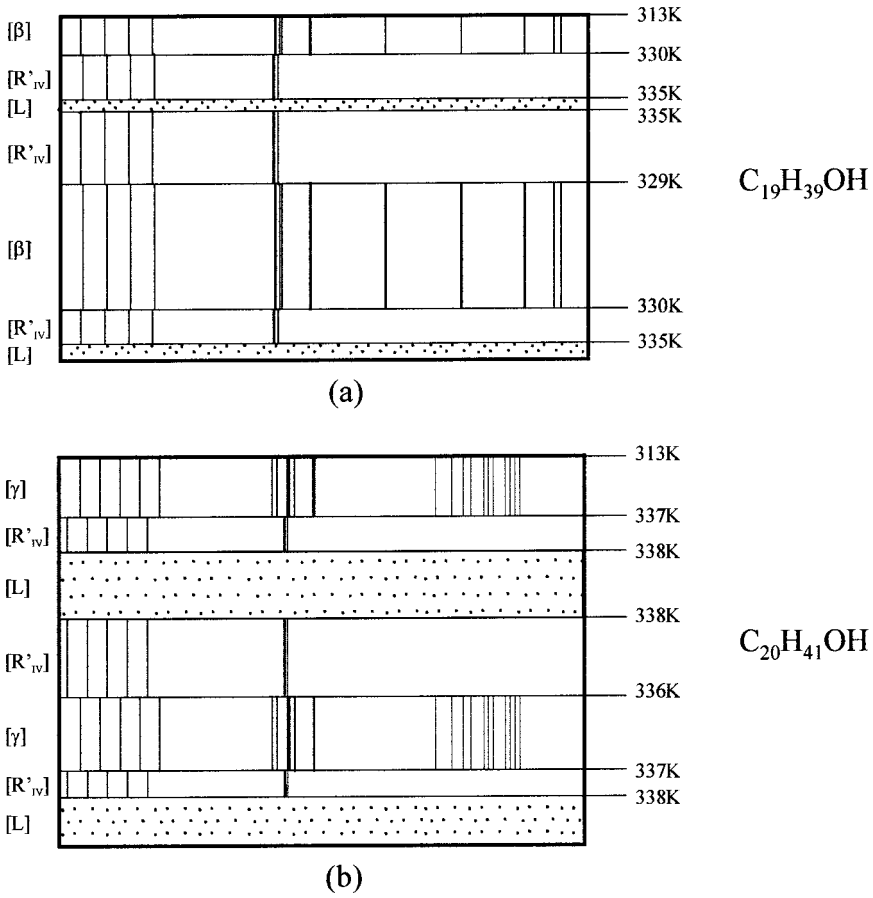

Figure 1. Scheme of Guinier-Simon photographs for $C_{19}H_{39}OH$ and $C_{20}H_{41}OH$.

FP84 sample-heating cell. The measurements for the quenched samples were made at 298 K after 1 h, 1 week, 1 month, and 3 months after the sample preparation. The position, half width, and relative intensity of each peak was determined, assuming it to be a Lorentzian function (the Gaussian contribution is negligible).

Infrared Spectroscopy. The infrared spectra were recorded by a Bomem DA3 FTIR spectrometer. All the samples were finely powdered and measured at room temperature using a diffuse reflection accessory (DRIFT), with the range of 450−4000 cm^{-1}. The resolution was 4 cm^{-1} and all spectra were run using the vacuum mode. The detector used was MCT (wide range); the beam splitter was KBr and the source a glow bar. Each spectrum was obtained by averaging 100 scans.

III. Results and Discussion

X-ray Powder Diffraction and Differential Scanning Calorimeter (DSC). The X-ray powder diffraction at room temperature showed that the commercial $C_{18}H_{37}OH$ and $C_{20}H_{41}OH$, those obtained by recrystallization from acetone or ether solution, and those recrystallized from the melt using a slow rate cooling (2 K·min^{-1}) process display the same γ-phase ($A2/a$) at room temperature. The commercial and recrystallized $C_{17}H_{35}OH$, however, showed a β-phase ($P2_1/c$) at room temperature. Our results of $C_{19}H_{39}OH$ showed that it is isostructural to $C_{17}H_{35}OH$. The refined cell parameters for these γ and β phases are given in Table 1 where, as can be seen, our results are in agreement with other studies.

When the γ-phase and β-phase are heated in the Guinier-Simon camera, they follow a similar change. Both phases transform to a rotator phase and it is this phase that melts, as is shown for $C_{19}H_{39}OH$ and $C_{20}H_{41}OH$ in Figure 1. The rotator phases were characterized by X-ray powder diffraction at different temperatures. The obtained patterns of the four *n*-alkanols studied were adjusted with the $C2/m$ symmetry and not with the hexagonal symmetry, so the rotator phase is assumed as R'_{IV} phase, which agrees with the result of Seto.[5] The cell parameters are summarized in Table 2.

The heating and cooling processes were also studied by DSC. On heating, the solid−solid transitions are

Table 1. Cell Parameters for γ Phase ($A2/a$, $Z = 8$) and β Phase ($P2_1/c$, $Z = 8$) at 298 K

	phase	*a* (Å)	*b* (Å)	*c* (Å)	β (deg)	ref
$C_{17}H_{35}OH$	β	5.031(3)	7.403(3)	94.52(4)	91.11(4)	this work
		5.03(2)	7.40(3)	94.6(3)	91.3(3)	5
$C_{18}H_{37}OH$	γ	9.031(3)	4.959(3)	98.19(5)	122.41(5)	this work
		8.96(3)	4.93(2)	99.7(3)	122.1(5)	5
		9.00	4.98	98.4	122.02	7
		8.998(5)	4.940(2)	98.01(4)	122.59(2)	8
$C_{19}H_{39}OH$	β	5.023(3)	7.335(3)	104.77(3)	91.11(2)	this work
$C_{20}H_{41}OH$	γ	9.035(3)	4.970(4)	108.71(9)	122.82(4)	this work
		9.02	4.97	122.14	108.52	7
		8.997(10)	4.932(4)	108.32(17)	122.86(4)	9

Table 2. Cell Parameters for Rotator Phase R'_{IV} ($C2/m$, $Z = 4$)

	a (Å)	*b* (Å)	*c* (Å)	β (deg)	ref
$C_{17}H_{35}OH$	8.414(6)	4.854(3)	46.61(3)	94.18(5)	this work (324 K)
	8.40	4.85	46.6	95.33	5
$C_{18}H_{37}OH$	8.458(3)	4.933(4)	48.58(6)	92.10(1)	this work (329 K)
	8.44	4.87	49.1	93.0	5
$C_{19}H_{39}OH$	8.419(6)	4.825(6)	50.92(3)	93.11(4)	this work (330 K)
$C_{20}H_{41}OH$	8.450(5)	4.940(7)	53.24(8)	93.70(2)	this work (335 K)

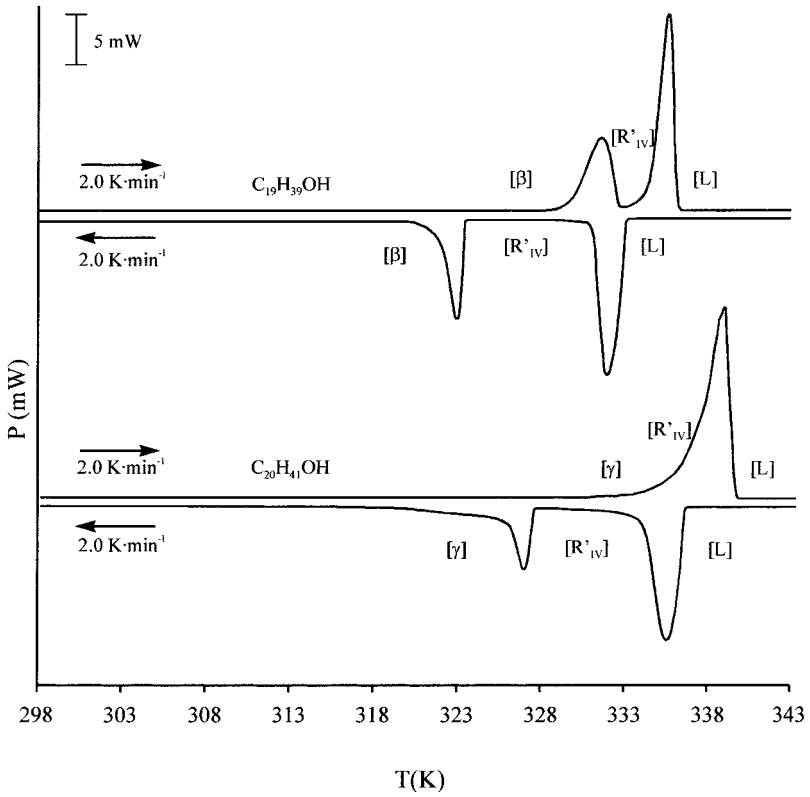

Figure 2. DSC analysis of commercial $C_{19}H_{39}OH$ and $C_{20}H_{41}OH$.

Table 3. Temperatures and Enthalpies of Transition and Melting of $C_{17}H_{35}OH$, $C_{18}H_{37}OH$, $C_{19}H_{39}OH$, and $C_{20}H_{41}OH$ on Heating at Normal Pressure

	solid−solid transition			solid−liquid transition			
	phases	T (K)	ΔH (kJ·mol^{-1})	$T_{R'IV\rightarrow L}$ (K)	$\Delta H_{R'IV\rightarrow L}$ (kJ·mol^{-1})	ΔH_{total} (kJ·mol^{-1})	ref
$C_{17}H_{35}OH$	$\beta\rightarrow R'_{IV}$	323.3 ± 0.5	25.2 ± 0.6	326.6 ± 0.5	37.0 ± 1.0	62.2	this work
		322		326			25
		322.8 ± 0.2	29	326.2 ± 0.2	35	64	26
$C_{18}H_{37}OH$	$\gamma\rightarrow R'_{IV}$	329.5 ± 0.5	26.5 ± 1.8	330.3 ± 0.5	40.1 ± 1.0	66.6	this work
		330.3		331.6			23
		328.5 ± 0.3	18.8 ± 0.8		39.2 ± 0.8	58.0	24
		330		331			25
		330.0 ± 0.2	26	331.0 ± 0.2	43	69	26
		330.6 ± 0.1	25.6	331.2 ± 0.1	41.1	66.7 ± 0.2	27
$C_{19}H_{39}OH$	$\beta\rightarrow R'_{IV}$	329.7 ± 0.9	29.1 ± 0.6	333.9 ± 0.5	43.3 ± 1.0	72.4	this work
		331 ± 0.1		334.5 ± 0.1		72.4 ± 0.1	27
$C_{20}H_{41}OH$	$\gamma\rightarrow R'_{IV}$	335.5 ± 0.5	28.4 ± 0.4	336.6 ± 0.5	43.6 ± 1.3	72.0	this work
		335.1		338.1			23
		332.0 ± 0.3	16.0 ± 0.8	339.6 ± 0.3	41.9 ± 0.8	57.9	24
		337.0 ± 0.1		338.2 ± 0.1		73.7 ± 0.2	27

overlapped with solid−liquid phenomena (mainly the $\gamma \rightarrow$ rotator transition in even alkanols), whereas on cooling the crystallization and transition are clearly separated. Due to the overlapping, the temperatures and enthalpies of melting were obtained in a second heating of the sample from a temperature above the solid−solid transition. A scheme of the DSC for $C_{19}H_{39}OH$ and $C_{20}H_{41}OH$ is shown in Figure 2. From the thermal hysteresis and the volume change in the transition, it is concluded that the transition of β or γ phases to rotator phase is a first-order transition according to ref 26. The enthalpy change involved in this solid−solid transition is about two-thirds of the melting enthalpy, whereas in the *n*-alkanes where only van der Waals interactions between the molecules are present, one-third of the melting enthalpy is involved. The temperatures and enthalpies of transition and melting determined by DSC are listed in Table 3, which are compared with other values obtained on a heating process.[23−27]

The quenched samples were measured in the Siemens D-500 at room temperature. For $C_{17}H_{35}OH$ and $C_{19}H_{39}OH$ the same β-phase ($P2_1/c$) is observed. Whereas for $C_{18}H_{37}OH$ and $C_{20}H_{41}OH$, the X-ray powder patterns reveal a mixture of γ and another phase, the latter in a

(23) Pradhan, S. D.; Katti, S. S.; Kulkarni, S. B. *Indian J. Chem.* **1970**, *8*, 632.
(24) Kuchhal, Y. K.; Shukla, R. N.; Biswas, A. B. *Thermochim. Acta* **1979**, *31*, 61.
(25) Yamamoto, T.; Nozaki, K.; Hara, T. *J. Chem. Phys.* **1990**, *92*, 631.
(26) Reuter, J.; Würflinger, A. *Ber. Bunsen-Ges. Phys. Chem.* **1995**, *99*, 1247.
(27) Van Miltenburg, J. C.; Oonk, H. A. J.; Ventolà, L. *J. Chem. Eng. Data* **2001**, *46*, 90.

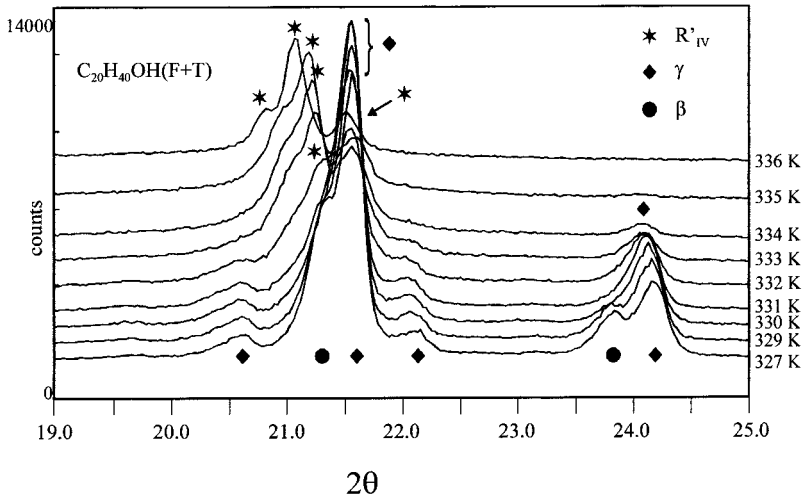

Figure 3. X-ray powder diffraction of quenched (F + T) $C_{20}H_{41}OH$ immediately after sample preparation.

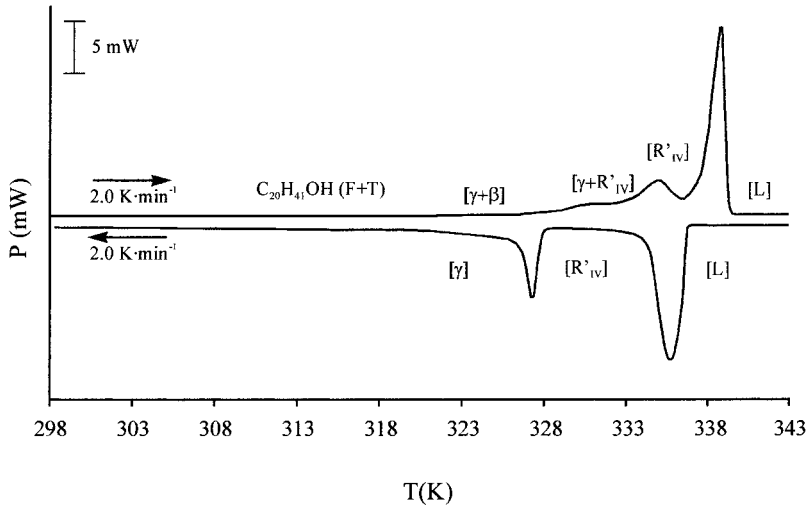

Figure 4. DSC analysis of quenched (F + T) $C_{20}H_{41}OH$ immediately after sample preparation.

minor proportion. The overlapping of reflections made the refinement of the cell-parameters difficult for the second phase, but the observed reflections could be properly indexed as 00*l*, 020, and 200 taken on the β-phase monoclinic ($P2_1/c$) observed in the odd *n*-alkanols. The cell-parameters have been estimated assuming an averaged β-angle from ref 6. The cell parameters for the β-phases are $a = 5.05$ Å, $b = 7.38$ Å, $c = 101.24$ Å, and $\beta = 91.35°$ for $C_{18}H_{37}OH$ and 5.01 Å, 7.32 Å, 107.41 Å, and 91.1° for $C_{20}H_{41}OH$. These results agree with Precht.[6] The study by powder diffraction in a heating process on the quenched samples of two even *n*-alkanols showed that the β-phase changes to the R'_{IV} phase at a lower temperature than the γ-phase, which shows that the β-phase is a metastable one. This is shown in Figure 3 for quenched $C_{20}H_{41}OH$ and the thermal analysis of this sample is shown in Figure 4; the temperature of the transition β-phase to R'_{IV} phase is about 329 K, whereas the transition γ-phase to R'_{IV} phase takes place at 335.5 K. This metastable β-phase remains at room temperature at least for three months after the quenching process was made.

Raman Scattering and Infrared Spectroscopy. The vibration mode assignments of the Raman spectra of $C_{17}H_{35}OH$, $C_{18}H_{37}OH$, $C_{19}H_{39}OH$, and $C_{20}H_{41}OH$ were made from both the vibrational spectra studies for the *n*-alkanes[12,28−30] and the crystal structures.[5,8,9] Following Snyder,[28,29] in discussing the spectra of these molecular compounds, it is useful to classify the vibrations in the following:

(1) External modes ($\nu < 50$ cm^{-1}) that give information about the packing forces.

(2) Internal modes, whose frequencies are dependent in some way on chain length, tend to overlap each other and blend into the background absorption with increasing chain length.

(3) Internal modes of nearly constant frequency which have intensities that decrease with increasing chain length. They are associated with motion in the ends of the chains.

(4) Finally, internal mode bands of nearly constant frequency whose intensities also tend to remain independent of chain length. These last bands are of little interest, because they yield no information about the structure.

(28) Snyder, R. G.; Schachtschneider, J. H. *Spectrochim. Acta* **1963**, *19*, 85; Schachtschneider, J. H.; Snyder, R. G. *Spectrochim. Acta* **1963**, *19*, 117.
(29) Snyder, R. G. *J. Chem. Phys.* **1967**, *47*, 1316.
(30) Zerbi, G.; Magni, R.; Gussoni, M.; Moritz, K. H.; Bigotto, A.; Dirlikov, S. *J. Chem. Phys.* **1981**, *75* (7), 3175.

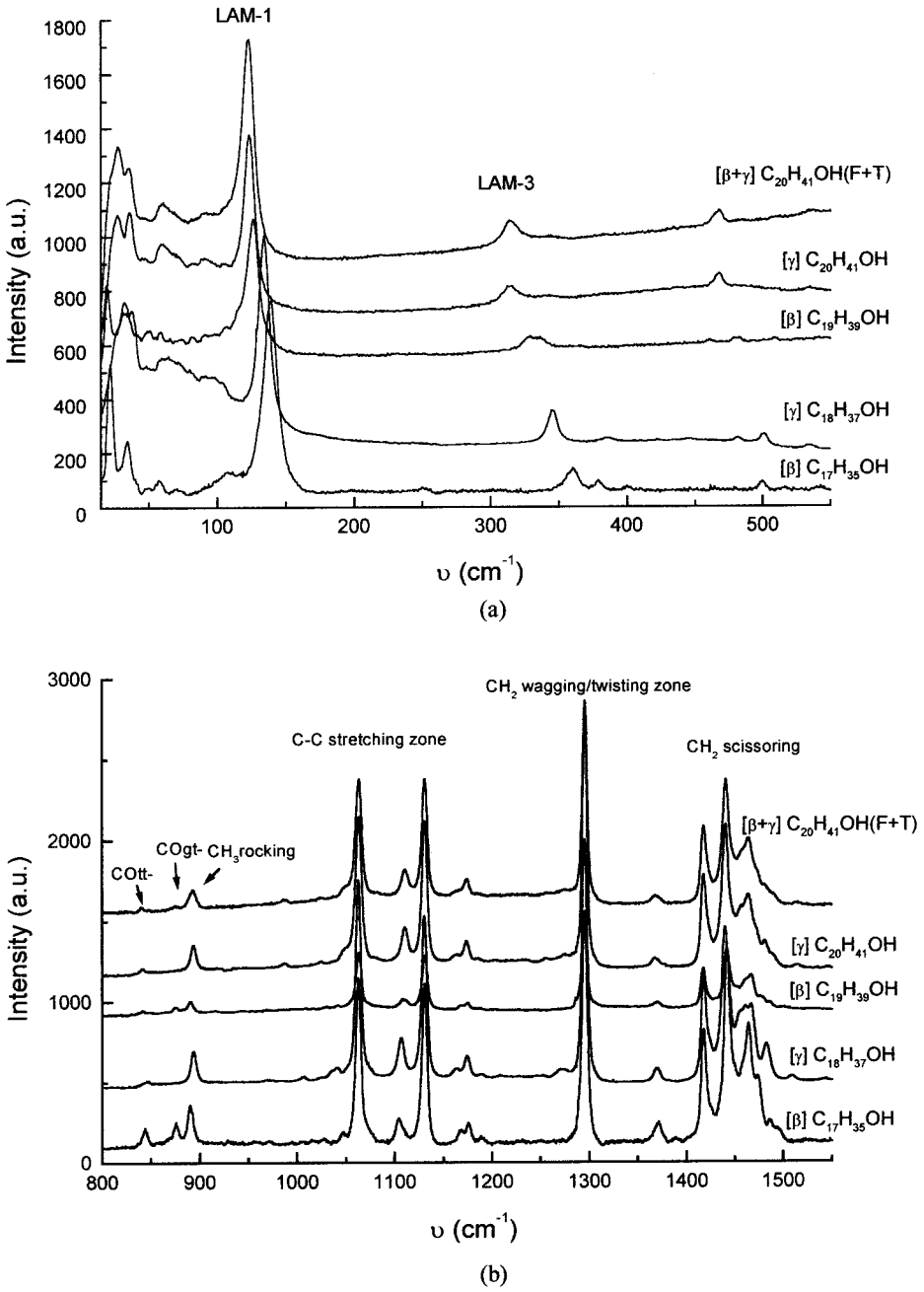

Figure 5. The 15−550 cm^{-1} range (a) and 850−1550 cm^{-1} range (b) of Raman scattering at 298 K of $C_{17}H_{35}OH$, $C_{18}H_{37}OH$, $C_{19}H_{39}OH$, $C_{20}H_{41}OH$, and measured 1 month after quenching (F + T) $C_{20}H_{41}OH$.

***β*- and *γ*-Phases.** The main frequencies of phonon modes of the Raman spectra measured at 298 K for commercial $C_{17}H_{35}OH$, $C_{18}H_{37}OH$, $C_{19}H_{39}OH$, and $C_{20}H_{41}$-OH are shown in Figure 5a,b.

The external modes of $C_{17}H_{35}OH$ and $C_{19}H_{39}OH$ on one hand, and $C_{18}H_{37}OH$ and $C_{20}H_{41}OH$ on the other hand, are similar (Figure 5a), which agrees with the isostructurallity shown from the X-ray powder diffraction data.

Internal modes whose frequencies are dependent on the chain length are the longitudinal acoustic modes (LAM). The frequency of these bands is specific for a chain with a certain number of carbon atoms. The observed bands are the LAM-1 and LAM-3 (Figure 5a). Above all, it is the frequency of the LAM-3 that most varies with the chain length.

Internal modes with practically constant frequency whose intensities decrease when increasing the chain length are in the CH_2 rocking mode zone ($700 < \nu < 1000$ cm^{-1}). According to Snyder,[28,29] in this zone we observe bands assigned to movements of the ends of the chains. In the spectra of the four *n*-alkanols (Figure 5b) we observed a band (about 890 cm^{-1}) assigned to CH_3 rocking of a chain with all trans conformation in the *n*-alkanes. In *β*-phase spectra of the two odd *n*-alkanols a new band appears at 875 cm^{-1} that could be assigned to CO gt- (gauche) mode, since the structure of this *β*-phase showed the presence of molecules with this form. Another band observed in the four *n*-alkanols at 845 cm^{-1} was assigned to CO tt- (trans). In this zone we can observe bands assigned by Snyder[28,29] to kink defects (CC -gtg′- at 850 cm^{-1}) and end gauche defects

(CC gt- at 870 cm^{-1}), but these conformations are not observed in the crystal structure of the γ-phase or in the β-phase at room temperature.[5,8,9]

The internal modes with nearly constant frequency and intensity are those of C−C stretching mode zone ($1000 < \nu < 1150$ cm^{-1}) and CH_2 wagging/twisting mode zone ($1150 < \nu < 1400$ cm^{-1}); this last zone can be important because these bands can indicate some kind of structural disorder according to Snyder.[28] But the frequency, intensity, and width are nearly constant in the four Raman spectra (Figure 5b), which agrees with single-crystal X-ray diffraction results,[5,8,9] where no disorder relating to chain localization is shown.

If the IR-spectra of β-phase and γ-phase of *n*-alkanols studied are compared with those observed in all-trans *n*-alkanes,[12] three broad new bands are observed and assigned to OH bending out of plane, OH bending in the plane, and OH stretching. Figure 6a−c shows as example the IR-spectra of the β-phase of $C_{19}H_{39}OH$ and the γ-phase of $C_{20}H_{41}OH$ at 298 K. The OH bending out of plane and OH bending in plane bands appear at 686 cm^{-1} and 1406 cm^{-1} in β-phase and at 606 and 1425 cm^{-1} in γ-phase respectively (Figure 6a,b). The OH stretching vibration (Figure 6c) is a broad band in the two phases, about 3300 cm^{-1} in β-phase while in γ-phase two bands are observed about 3230 and 3330 cm^{-1}. Other differences are observed in C−C stretching zone (Figure 6a) where the β-phase showed a strong band at 1122 cm^{-1}, while γ-phase showed two less-intense bands. In the CH_2 wagging/twisting zone of the spectra (Figure 6b), the β-phase showed more complexity absorptions than the γ-phase, but it did not show the bands at 1366 and 1353 cm^{-1} assigned by Maroncelli et al.[12] to CH_2 wagging adjoining to kink defects (CC -gtg′-) and a double gauche defect (CC -gg-). Finally a slight difference was observed in the CH_3 and CH_2 stretching zone (Figure 6c).

The different frequencies of these bands in the spectra of the two phases are consistent with the IR-results of ref 20 and the structural data.[5,8,9] In γ-phase the molecules are all trans conformation and hydrogen-bond spirals are formed along the a direction with the protons randomly distributed over two possible positions. In β-phase, molecules in all trans conformations alternate with molecules with CO gt- gauche conformation and the hydrogen bonds forming infinite chains along the screw axes; this coexistence of two molecules with different conformation logically implies differences in the OH vibrations and the existence of new bands in their spectra.

The Raman spectra of quenched samples and the X-ray powder diffraction results are coherent. The Raman spectra of quenched $C_{17}H_{35}OH$ and $C_{19}H_{39}OH$ show solely the β-phase. On the contrary, the spectra for quenched $C_{18}H_{37}OH$ and $C_{20}H_{41}OH$ show a mixture of two phases: the frequencies of their γ-phases coexist with the band assigned to the CO gt- gauche of the β-phase. The measurements realized after 1 h, 1 week, 1 month, and 3 months after the quenching showed no significant differences. In Figure 5a,b, we show as an example the results of a quenched $C_{20}H_{41}OH$ 1 month after the quenching process was made.

Both the IR and the Raman results are in agreement. In Figure 6a−c, we compare the IR spectra of β-phase of $C_{19}H_{39}OH$ and γ-phase of $C_{20}H_{41}OH$ with the IR spectra of a quenched $C_{19}H_{39}OH$ and quenched $C_{20}H_{41}OH$ at 298 K. Again in odd *n*-alkanols the results are the same, but in the quenched even *n*-alkanols we can observe the following differences:

(1) New bands appear in the CH_2 rocking mode zone ($700 < \nu < 1000$ cm^{-1}) between the k-odd rocking mode. Since the k-even modes are IR inactive for the all-trans chain, these bands must result from a nonplanar conformation.

(2) New band at 1122 cm^{-1} as it was observed in the β-phase of the odd *n*-alkanols.

(3) The intensity of the OH bending, mainly the OH bending in plane at 1425 cm^{-1} decreases in the quenched sample and a new band appears at 1406 cm^{-1}. This frequency is the same in β-phase of the odd *n*-alkanols.

(4) The CH_3 symmetric stretching (Figure 6c) of quenched $C_{20}H_{41}OH$ is similar to the β-phase of the odd *n*-alkanols.

Rotator Phase. Raman spectra were measured at different temperatures in order to compare and obtain structural information of the rotator phase of the four *n*-alkanols studied. Previous studies on the *n*-alkane family[12,28−30] show that the rotator phases are characterized by the rotation of the chain along its long axis and the existence of defects in the chain (kink and end gauche mainly).

Figure 7a,b shows the Raman spectra of the rotator phase for each alkanol obtained in the cooling process because the crystallization and transition are clearly separated. We observe that all the spectra of the *n*-alkanols studied are very similar, consistent with the same phase R'_{IV} characterized by X-ray powder diffraction data. The characteristic and significant differences between the spectra of low-temperature phases and the rotator phase are:

(1) The disappearance of external mode bands and a general broadening of all bands.

(2) A diminution of frequency and intensity of longitudinal acoustic modes (LAM).

(3) The existence of the band at 875 cm^{-1} assigned to CO gt- mode and a new band near 1083 cm^{-1}.

(4) The pass from four to two broader bands in the CH_2 wagging/twisting zone.

The rotation of the methylene chain along the chain axis produces changes in the structural packing and is consistent with a broadening of the bands. The variation in the LAM modes suggests the presence of gauche conformers at the end of the chain, which agrees with the existence of CO gt- form. The band near 1083 cm^{-1} was observed in the Raman spectra of polyethylenes. This band is best described as C−C stretching according to the potential-energy distribution computed by Snyder.[29] But in this band there is a significant contribution from CH_2 wagging and it is attributed to antisymmetric C−C stretching produced by the wagging of the methylene group adjoining gauche bonds. The variation in the CH_2 wagging/twisting zone suggests a disorder in the carbon chain in the high-temperature phase (variations in torsion angles concerning the theoretical C−C−C−C angle of 180° in a chain with all trans conformation). A similar behavior is observed in *n*-alkanes.[28] The bands assigned to

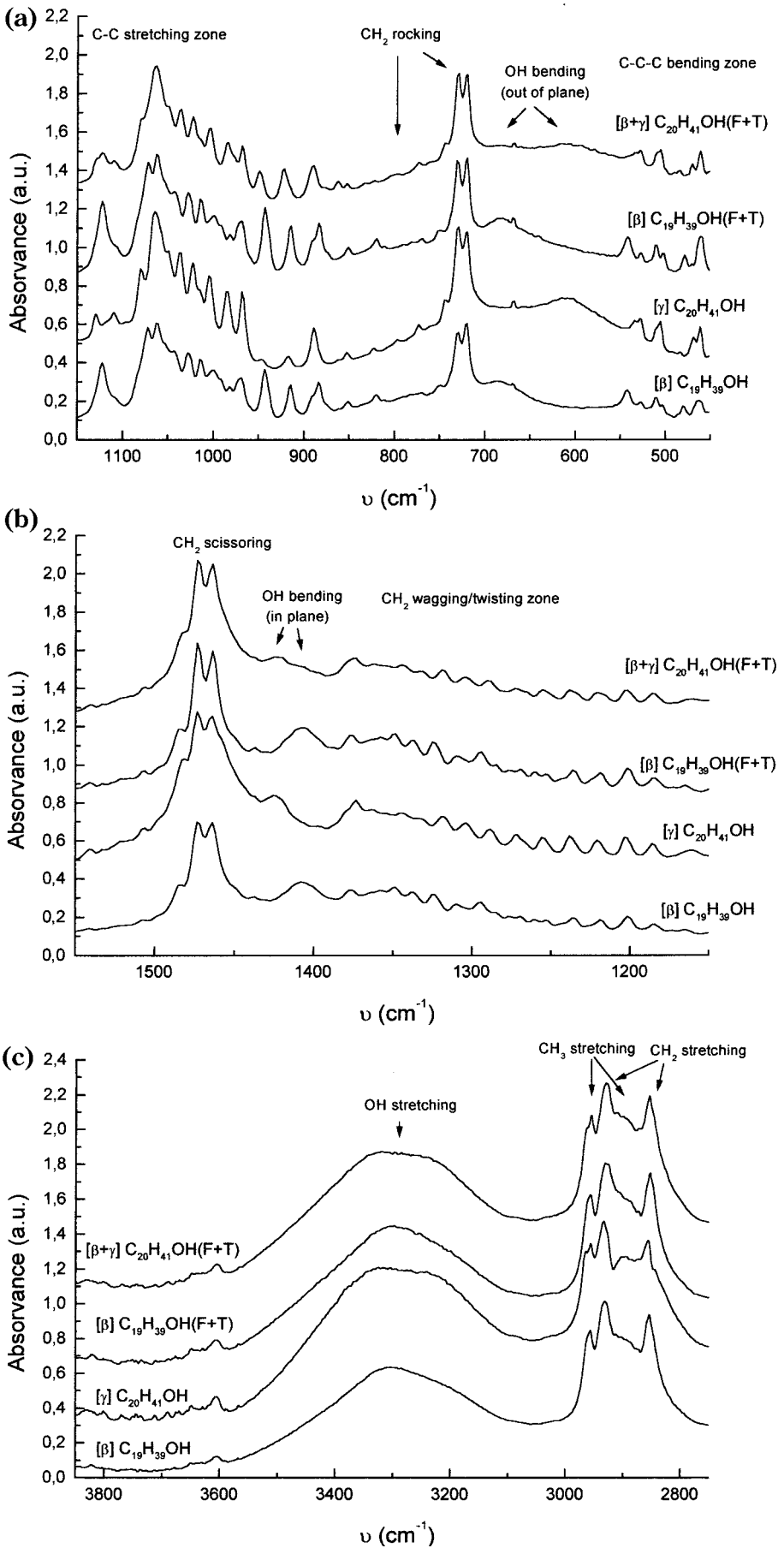

Figure 6. (a)−(c): Main zones of infrared spectra at 298 K $C_{19}H_{39}OH$, $C_{20}H_{41}OH$, quenched (F + T) $C_{19}H_{39}OH$ and measured 1 month after quenching (F + T) $C_{20}H_{41}OH$.

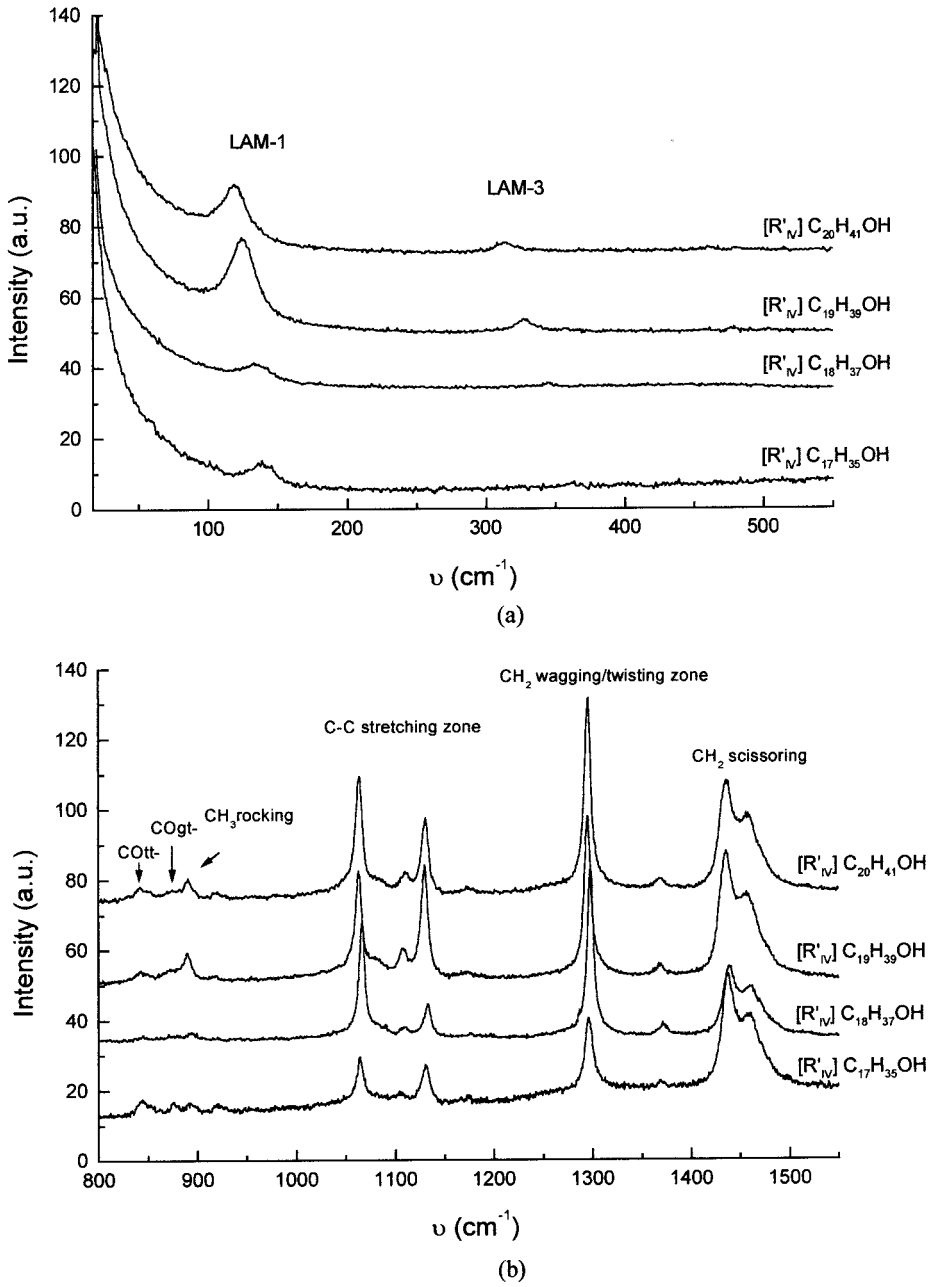

Figure 7. The 17−550 cm^{-1} range (a) and 850−1550 cm^{-1} range (b) of Raman scattering of rotator phase (R'_{IV}) of $C_{17}H_{35}OH$ (at 324 K), $C_{18}H_{37}OH$ (at 327 K), $C_{19}H_{39}OH$ (332 K), and $C_{20}H_{41}OH$ (at 332 K), measured on cooling.

kink defects and double gauche defects are not observed in the rotator phases with the Raman measurements.

Finally, our results are in agreement with those obtained by Ishikawa and Ando[11] by ^{13}C NMR spectroscopy on the 1-octadecanol. These authors formulated two conclusions: there is a slight variation in the CCCC forms from the γ-phase to the rotator phase, and the C atom linked to O atom is in two magnetically nonequivalent sites in the γ-phase. The second conclusion is in agreement with the disordered localization of the H atom linked to the O atom in the crystal structure of the γ-phase, but they did not observe the CO gt- (gauche form) in the rotator phase. According to our results, his assignment of C_{16} shift must be C_2' and the assignment of C_{4-15} must be a C_{4-16} shift.

IV. Conclusions

At room temperature the two odd *n*-alkanols $C_{17}H_{35}OH$ and $C_{19}H_{39}OH$ are isostructural, showing the same β-phase ($P2_1/c$, $Z = 8$). The comparison of their Raman and IR spectra showed that in both cases there is a coexistence of molecules with all trans conformation and molecules with CO gt- conformation. The two even *n*-alkanols $C_{18}H_{37}OH$ and $C_{20}H_{41}OH$ are also isostructural at 298 K showing only the γ-phase ($A2/a$, $Z = 8$) with only molecules in all trans conformation. The β-phase (in the odd *n*-alkanols) and γ-phase (in the even *n*-alkanols) are observed on the commercial substances, recrystallized samples from different solvents and on substances recrystallized by slow cooling from the melt.

If these odd *n*-alkanols are submitted to a quenching process the same β-phase ($P2_1/c$, $Z = 8$) is observed; whereas, in the two even *n*-alkanols, a mixture of γ-phase and β-phase is obtained. The results of X-ray powder diffraction as a function of temperature and the DSC analysis showed that this β-phase appearing in the quenched even *n*-alkanols is metastable but it could be observed at 298 K at least from three months after the quenching was made. According to the results from X-ray powder diffraction, Raman scattering, and IR spectroscopy the metastable β-phase of $C_{18}H_{37}OH$ and $C_{20}H_{41}OH$ is isostructural with the stable β-phase of $C_{17}H_{35}OH$ and $C_{19}H_{39}OH$.

These phases transform at higher temperatures to a monoclinic phase R'_{IV} ($C2/m$, $Z = 4$) by a first-order transition. This rotator phase shows CO gt- (end gauche) forms and a disorder in the carbon chain, which could explain the appearance of β-phase when a quenching process is followed from the melt in the even *n*-alkanols. The rotation of the carbon chain along the chain axis produces changes in the structural packing and explains the variations of the observed external modes.

Acknowledgment. The authors thank the Comisión Interministerial de Ciencia y Tecnología for financial support through Grant MAT97-0371.

Supporting Information Available: Two tables detailing the main frequencies of the phonon modes (PDF). This material is available free of charge via the Internet at http://pubs.acs.org.

CM011010H